https://doi.org/10.48048/tis.2023.6145

Magnetic Nanoparticles Coated with Cationic Polymer and Label-Free Peptide Aptamer for Selective Adsorption with Bisphenol A

Jakkrit Tummachote[1], Boonjira Rutnakornpituk[1,2] and Metha Rutnakornpituk[1,2,*]

[1]Department of Chemistry, Faculty of Science, Naresuan University, Phitsanulok 65000, Thailand
[2]Center of Excellence in Biomaterials, Faculty of Science, Naresuan University, Phitsanulok 65000, Thailand

([*]Corresponding author's e-mail: methar@nu.ac.th)

Received: 29 September 2022, Revised: 22 October 2022, Accepted: 28 November 2022, Published: 22 January 2023

Abstract

Magnetite nanoparticles coated with quaternized poly(diethylamino)ethyl methacrylate (PDEAEMA) (PQDEA@MNP) and functionalized with bisphenol A (BPA)-specific peptide aptamer (CKSLENSYC) were synthesized and used as nano-adsorbents for selective adsorption with BPA. The polymer coated on the particles provided their good stability and dispersibility in water, and the aptamer provided selective adsorption with BPA targets. Fourier transformed infrared spectrophotometry (FTIR), thermogravimetric analysis (TGA) and vibrating sample magnetometry (VSM) techniques confirmed the presence of the polymer on the particle surface. From transmission electron microscopy (TEM) study, the particle size was *ca*.6 - 10 nm in diameter with some nanoclustering (30 - 60 nm in diameter of the nanoclusters). The selective adsorption of BPA on the particles was predominant over the non-specific adsorption when performed in PBS buffer (pH 10) in the presence of NaCl and tween-20. The nano-adsorbents had a good linearity range for the detection of BPA between 0.04 and 0.20 ppm with limit of detection (LOD) of 0.0145 ppm. They retained good BPA adsorption efficiency even when other interfering molecules were present. This simple measurement with the use of these nano-adsorbents without molecular labelling might be promising solid supports for use in various applications with good tolerance towards interfering molecules.

Keywords: Magnetic, Nanoparticle, Aptamer, Bisphenol A, Nano-adsorbent

Introduction

Bisphenol A (BPA), also called 4,4′-dihydroxydiphenylpropane, is widely used as a starting reagent in the manufacture of polycarbonate and epoxy resins, the base materials in a variety of common consumer goods, e.g., water bottles, food cans and medical devices [1,2]. However, many studies showed that BPA caused various adverse health effects, such as male sexual dysfunction [3], heart disease [4], prostate and mammary gland cancers, diabetes and immune system alternations [5,6]. Under high-temperature and acidic condition, BPA was released into the environmental media from BPA-containing products [7,8]. It can enter the human body through various paths, resulting in a serious potential risk to human health. BPA has been banned from the use as baby bottles by the United States Food and Drug Administration in 2012 [9]. However, polycarbonate bottles remain permitted and are in prevalent use in Thailand. Therefore, to prevent these undesirable effects on food safety and human health, it is important to detect trace amounts of BPA with high sensitivity and selectivity approaches. Various techniques have been reported for BPA detections, e.g. UV spectrophotometry [10], high-performance liquid chromatography (HPLC) [11,12], gas chromatography-mass spectrometry (GC-MS) [13,14], electrochemical sensors [15-17], fluorescence analysis [18,19] and many others.

During the past few decades, the studies in magnetite nanoparticle (MNP) have gained a great attention as a potential nano-solid support owing to its large surface area, good biocompatibility, facile synthesis, and easy separation from dispersion with an assistance of a magnet. Moreover, an easy recovery and reuse for multiple cycles allowed it to be even more promising for further studies [20-23]. In particular, MNP coated with water dispersible polymers has various potential applications in a wide range of biomedical areas, e.g. targeted drug delivery [24-27], contrast agent for magnetic resonance imaging (MRI) [28], specific targeting for biosensing of cancer biomarker [29], DNA and RNA purification [30]. Because of its high surface-area-to-volume ratio and strong inter-particle attractive forces, such as Van der Waals force, magnetic force and gravitational force, it tended to aggregate and essentially form uncontrollable large cluster, leading to the loss in their desirable unique properties and limiting its applications [21,31,32].

Therefore, coating MNP with functional polymers, e.g., poly(acrylic acid) [33] and poly(diethylamino)ethyl methacrylate (PDEAEMA) [20] and thermo-responsive polymers, e.g. poly(N-isopropylacrylamide) [34], is one of efficient strategies to prevent this undesirable agglomeration. Long chain polymers coating on MNP surface provided its steric stabilization and this can be designed to improve its stability and dispersibility in the media [23,35-39]. In addition, the polymers coating on the particle surface can also serve as a platform for functionalization with bio-entities, e.g. creatinine [40], peptide and DNA [41-43]. For example, positively charged polymers such as poly(dimethylamino)ethyl methacrylate (PDMAEMA) and PDEAEMA grafted from MNP surface can be adsorbed with negatively charged DNA *via* electrostatic interaction and used for DNA extraction/isolation [44].

Aptamer is single-strand DNA, RNA or peptide that can bind specifically to target ions or molecules. It has recently attracted great attention in biosensor fabrications with high selectivity and high sensitivity for target detections [18,19,43,45,46]. Once approaching to the target, it folded into spatially stable structure, making it suitable for target binding by either complementary pairing, electrostatic interaction, Van der Waals force, hydrogen bonding or stacking [47]. In particular, there are many advantages using peptide as aptamer, e.g. high specificity to the target to mimic a hormone-receptor interaction, low-cost and easy to be synthesized as compared with other biomolecules. However, the research involving the use of peptide aptamer for specifically binding with BPA has barely been reported [18,46]. These reports indicated that peptide aptamer had high selectivity and sensitivity for BPA detection.

In this work, aptamer-immobilized magnetic nano-adsorbents were synthesized and used for selective adsorption with BPA (**Figure 1**). The magnetic nano-adsorbents, called PQDEA@MNP, comprised MNP that well responded to an external magnet to facilitate the particle separation, and quaternized PDEAEMA coating on MNP to improve its stability and dispersibility in water. Importantly, this positively charged polymer served as a platform for immobilization with negatively charged aptamer through ionic interaction. The peptide having CKSLENSYC sequence was used as BPA-specific aptamer in this work because it has been previously reported to be able to specifically interact with BPA [48,49]. Various characterization techniques, e.g. fourier transformed infrared spectrophotometry (FTIR), thermogravimetric analysis (TGA), vibrating sample magnetometry (VSM) and transmission electron microscopy (TEM), were used to investigate the properties of the particles. Adsorption condition of BPA on the aptamer-free particles was investigated aiming to minimize the undesirable non-specific adsorption between BPA and the particle surface. Adsorption performance of aptamer-immobilized particles with BPA, e.g. detection of limit (LOD), selectivity and tolerance to interfering molecules, was also investigated.

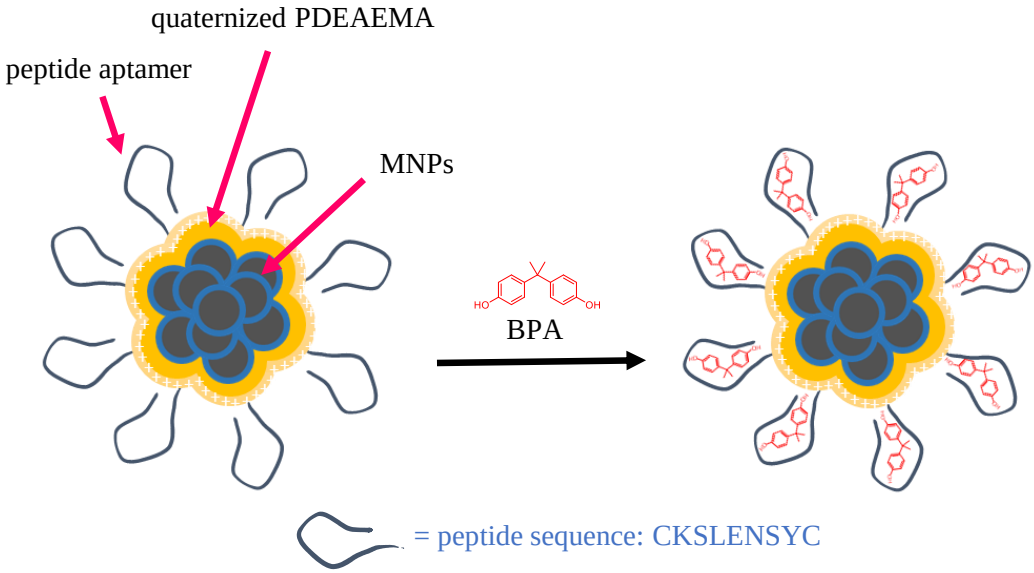

Figure 1 The proposed mechanism for selective adsorption of BPA with aptamer-immobilized PQDEA@MNP as nano-absorbents.

Materials and methods

Materials

Otherwise stated, all reagents were used as received; iron(III) chloride ($FeCl_3.6H_2O$) (98 %, Acros Organics), iron (II) chloride tetrahydrate ($FeCl_2.4H_2O$) (99 + %, Acros Organics), ammonia solution 30 % (NH_4OH) (Carlo Erba), oleic acid (Carlo Erba), 3-(trimethoxysily)propyl methacrylate (TMSPMA) (98 %, Aldrich), 2-2′-azobis(2-methylpropionitrile) (AIBN) (98 %, Sigma-Aldrich), 2-(diethylamino)ethyl methacrylate (DEAEMA) (Aldrich), iodomethane stabilized with silver (CH_3I) (Merck), 2,2-bis(4-hydoxyphenyl)-hexafluoropropane (BPAF) (TCI), 4,4′-dihydroxybiphenyl (DHBP) (TCI), bis(4-hydroxyphenyl) Sulfone (BPS) (TCI), bisphenol A (BPA) (99 %, Aldrich), n-hexane (Carlo Erba), triethylamine (TEA) (Merck), tetrahydrofuran (THF) (RCI labscan), acetonitrile (ACN) (RCI labscan), acetone (RCI labscan), toluene (RCI labscan), tris(hydroxymethyl)-aminomethane (tris-HCl) (99.5 %, Carlo Erba), sodium Chloride (NaCl) (99 % RCI Labscan), potassium dihydrogen orthophosphate (KH_2PO_4) (99.7 %, Fisher Scientific), potassium phosphate dibasic (K_2HPO_4) (Carlo Erba). Peptide aptamer (CKSLENSYC, 97.6 %, Lot: U373GFG160-3) was synthesized by GenScript Biotech Corporation (Nanjing, China). Dioxane (RCI Labscan) was dried in molecular sieves prior to use.

Instrument

Fluorescence intensity was obtained using high performance liquid chromatography with fluorescence detector (HPLC-FLD), (1260 series, Agilent), equipped with an autosampler, a quaternary pump and a thermostat column compartment. The excitation and emission wavelengths were 229 and 315 nm, respectively [43]. A Vertical UPS C18 column (250×4.6 nm^2, 5 µm) and a guard-column were used for all HPLC analyses. The column temperature was kept at 25 ºC and the injection volume was 20 µL. For all analyses, a gradient condition was used at the flow rate of 1.0 mL/min, by combining solvent A (water) and solvent B (acetonitrile): 50 % B from 0 to 9 min (isocratic elution for the sample analyses); 50 - 100 % B from 9 to 12 min (for cleaning the column); 100 - 50 % B from 12 to 15 min (for equilibrating the column). All samples were diluted with 30 % acetonitrile to enhance the fluorescence intensity. TEM analysis (Tecnai 12, Philips TEM) was operated at 120 kV and equipped with a Gatan model 782 CCD camera. The particles were redispersed in ethanol and sonicated prior to deposition on a TEM grid. FTIR was performed *via* fourier transform infrared spectrometer (FTIR) (Spectrum GX, Perkin Elmer). The FTIR samples were dried *in vacuo* and used ATR mode as the sample preparation method. Size and zeta potential values were measured *via* Zetasizer, Nano ZS4700, Malvern. Magnetic properties were performed *via* vibrating sample magnetometer (VSM) using a magnetic moment in range of ±10,000 G of the applied magnetic fields. Thermogravimetric analysis (TGA) was operated at the temperature ranging between 25 and 600 ºC and a heating rate of 20 ºC/min under nitrogen atmosphere.

Synthesis of PQDEA@MNP

The mixture of $FeCl_3.6H_2O$ (1.66 g, 6.14×10^{-3} mol) and $FeCl_2.4H_2O$ (1.00 g, 5.03×10^{-3} mol) in deionized water (20 mL) was stirred at room temperature for 30 min. Black precipitate was observed once 25 % NH_4OH (20 mL) was added into the solution (**Figure 2**). After stirring for 30 min, MNP was magnetically separated and washed with deionized water. An oleic acid solution (2.0 mL in 20 mL toluene) was added into the MNP dispersion while stirring for 30 min to obtain oleic acid-coated MNP. The particles were re-precipitated in acetone and then dried *in vacuo*. Zero point five g of the dried particles was redispersed in toluene (20 mL), followed by an addition of TEA in a round bottom flask. TMSPMA (5.15 mL, 2.1×10^{-2} mol) was then added dropwise to the mixture and it was stirred for 24 h at room temperature under N_2 atmosphere to obtain methacrylate-coated MNP (MA@MNP). The particles were precipitated in hexane, magnetically separated, and washed with hexane and then dioxane. MA@MNP (0.02 g dispersed in 4.4 mL of dioxane) was copolymerized with DEAEMA (1.22 mL, 6.1×10^{-3} mol) using an AIBN radical initiator (0.01 g, 6.1×10^{-5} mol in 1.0 mL of dioxane). The reaction was performed at 70 ºC for 30 min under N_2 atmosphere. After magnetic separation, washing with dioxane and drying, PDEAEMA-coated MNP (PDEA@MNP) was obtained. In the quaternization step, methyl iodide (1.0 mL, 6.4×10^{-2} mol) was added to the particle dispersion (20.0 mg in 1.0 mL of THF) and the mixture was sonicated for 3 h in the dark at 25 ºC. The quaternized PDEA@MNP (PQDEA@MNP) (45 % yield) was magnetically separated, washed with water, and stored as the dispersion in deionized water (20.0 mL).

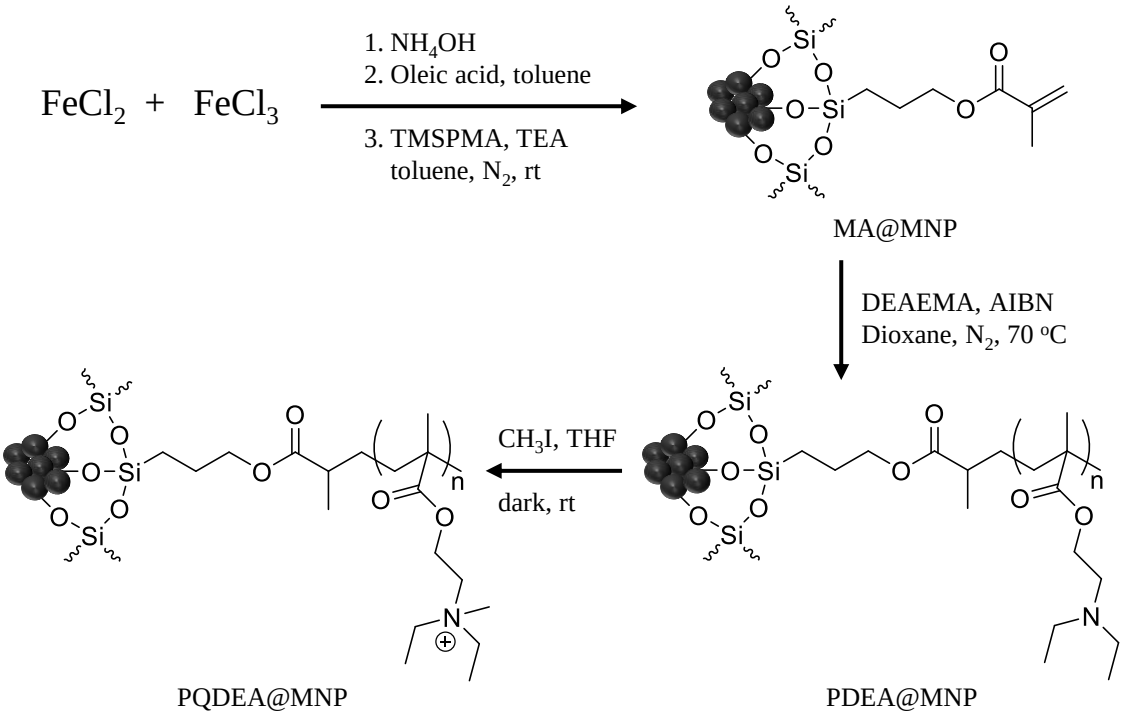

Figure 2 The scheme for the synthesis of PQDEA@MNP nano-adsorbent.

Preparation of BPA and aptamer stock solutions

A BPA stock solution was prepared to obtain the BPA concentration of 200 ppm in deionized water. BPA was sonicated for 1 h at 70 ºC using ultrasonic frequency of 37 kHz (Elmasonic S 70) to allow the complete solubility of BPA in water. The BPA standard solutions having various concentrations including 0.02, 0.04, 0.08, 0.12, 0.16 and 0.20 ppm were prepared by sequential dilution of the BPA stock solutions with various buffer solutions, such as phosphate buffer (PBS, 10 mM) and tris-HCl buffer (50 mM) with and without 150 mM NaCl and 0.1 % tween-20. The aptamer stock solution (CKSLENSYC) was prepared to have the aptamer concentration of 4000 ppm in deionized water and stored at –20 ºC in a refrigerator.

Measurement of adsorbed BPA on the particles

The mixture of PQDEA@MNP (0.25 mg) and the aptamer stock solution (10 µL) was added to a 50 µL of the BPA stock solution, and then the total volume was adjusted to 500 µL with buffer solution (**Figure S1** in Supporting information). After stirring for 5 min, the mixture was placed on a magnet to separate PQDEA@MNP from the dispersion. Finally, the fluorescence intensity of the supernatant was quantitatively analyzed *via* HPLC-FLD from the standard curves. The adsorbed BPA on the particles was calculated from the difference of the loaded and the unadsorbed BPA remaining in the supernatant.

Results and discussion

Characterization of MNP

FTIR spectra of MNP in each step of the reactions are shown in **Figure 3**. FTIR spectrum of bare MNP exhibits the characteristic peak at 548 cm^{-1} of Fe-O bond (**Figure 3**(**A**)). Those of MA@MNP show the signals of C=O stretching (1696 cm^{-1}), C=C stretching (1630 cm^{-1}), C-O stretching (1168 cm^{-1}) and Si-O bond (968 cm^{-1}) (**Figure 3**(**B**)) [22,50,51]. The spectrum of PDEA@MNP shows the strong signals of C=O stretching (1721 cm^{-1}) due to the ester linkage in PDEAEMA, as well as those of C-O stretching (1145 cm^{-1}), Si-O (964 cm^{-1}) and C-N (998 cm^{-1}) (**Figure 3**(**C**)). This information signified the coating of MNP with PDEAEMA. The spectrum of PQDEA@MNP was similar to those of PDEA@MNP as shown in **Figure 3**(**D**). The proposed mechanism of the silica layer formation on MNP surface is shown in **Figure S2** in Supporting information. Briefly, the reaction between Fe-O^- on MNP surface and TMSPMA took place, followed by the reaction of TMSPMA-immobilized MNP with water to form silanols, and finally the repetitive reactions between 2 neighboring silanols to form silica layer on MNP surface [20,22].

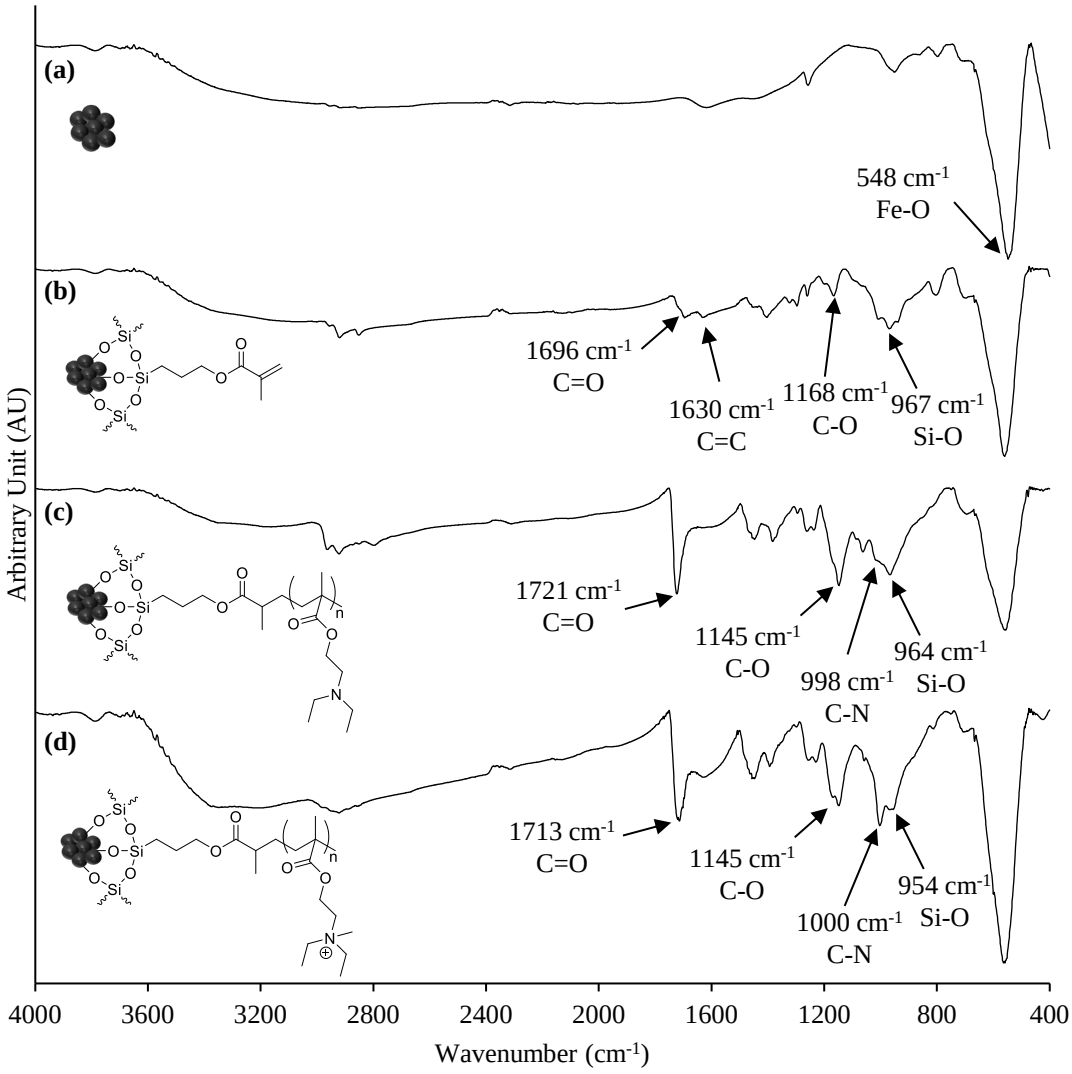

Figure 3 FTIR spectra of (a) bare MNP, (b) MA@MNP, (c) PDEA@MNP and (d) PQDEA@MNP.

TGA technique was used to determine the percentages of the polymer coating on the particles with an assumption that the weight residue was MNP core, and the weight loss was organic composition including polymer. Fourteen % weight loss of bare MNP in **Figure 4**(**a**) was probably due to the organic residue presenting on the thin layer of the particles, e.g. oleic acid (thermogram (1) in **Figure 4**(**a**)) [35,36,37]. The weight loss of PDEA@MNP was *ca*.27 % and those of PQDEA@MNP was *ca*.29 % (*ca*.71 - 73 % of MNP core in the nanocomposites). The slight increase in the weight loss in PQDEA@MNP when compared with PDEA@MNP was attributed to the additional methyl groups presenting in the polymer structure after the quaternization (thermogram (2) and (3) in **Figure 4**(**a**)). These results corresponded well to those obtained from VSM technique (**Figure 4**(**b**)). The slight decrease in the saturation magnetization values (M_s) from 55 emu/g of PDEA@MNP (curve (2) in **Figure 4**(**b**)) to 46 emu/g of PQDEA@MNP (curve (3) in **Figure 4**(**b**)) signified the increase of the non-magnetic components in the particles after the quaternization. It should be noted that M_s values of bare MNP was 69 % as shown in curve (1) in **Figure 4**(**b**).

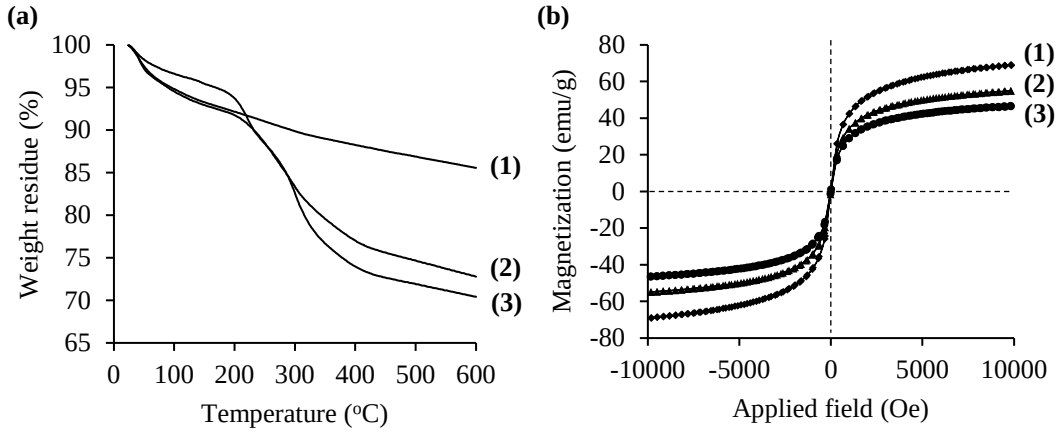

Figure 4 (a) TGA thermograms and (b) *M-H* curves of (1) bare MNP, (2) PDEA@MNP and (3) PQDEA@MNP.

The particle size and its distribution of MA@MNP and PQDEA@MNP were investigated *via* TEM technique (**Figure 5**). It should be noted that bare MNP cannot be observed *via* TEM due to the lack of particle dispersibility in water. MA@MNP showed the particle size of *ca*.6 - 10 nm with some nanoclustering with the size range of 50 - 150 nm. After the polymerization and then quaternization, PQDEA@MNP exhibited some improvement in their water dispersibility as indicated by the smaller size of the nanoclusters (30 - 60 nm in diameter), and this was attributed to the coating of the hydrophilic polymers on the MNP surface.

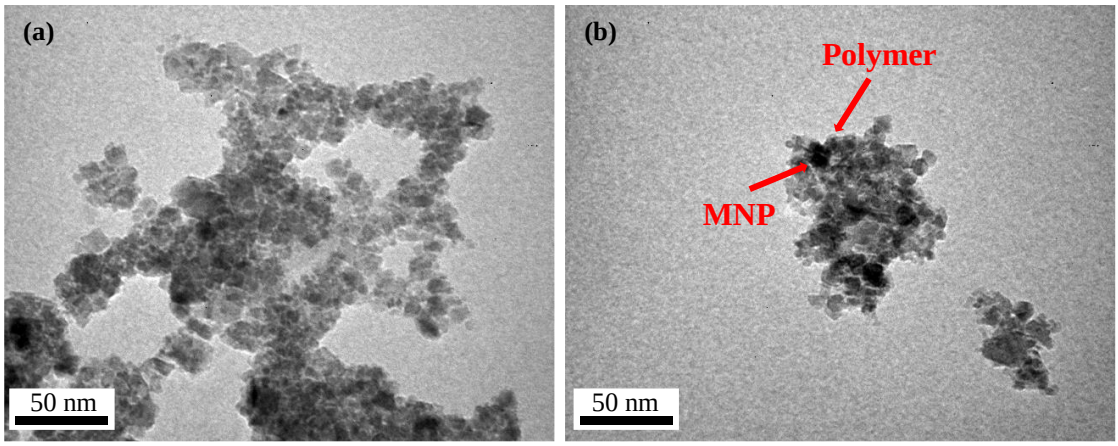

Figure 5 TEM images of (a) MA@MNP and (b) PQDEA@MNP.

The particles with good dispersibility and high stability in water while retaining their good magnetic responsiveness were much desirable. However, the response to magnetic field of the individual particles was so low that they were troublesome for magnetic separation from the dispersion. The formation of the nanoclusters with controllable degrees of clustering was necessary because this can increase the magnetic responsiveness of the particles, while their good water dispersibility was retained. The ratio of MA@MNP to DEAEMA used in the polymer coating step was crucial. In this work, the reaction between 0.02 g of MA@MNP and 1.22 mL of DEAEMA (100:1 equivalent ratio of DEAEMA:AIBN initiator) in 4.4 mL of dioxane was used in the polymer coating step and this condition gave rise to those with desirable properties. After the quaternization of these particles, PQDEA@MNP were obtained and their stability in water and magnetic separation ability are shown in **Figure S3** in Supporting information. They were well dispersible in water without visually noticeable aggregation after 5 h of standing and can be magnetically separated within 3 - 5 min.

Investigation of the proper adsorption condition of BPA on aptamer-free PQDEA@MNP to minimize non-specific adsorption

The objective of this work was to study the adsorption selectivity of BPA with aptamer-immobilized PQDEA@MNP. Therefore, non-specific adsorption of BPA on the particle surface is undesirable and needed to be minimized, and this can facilitate the selective adsorption of BPA and aptamer immobilized on the particles. This non-specific adsorption was assumed due to the physical adsorption of hydrophobic moiety between BPA and the coating polymer [52,53]. This experiment was designed to determine the proper condition such that BPA adsorption owing to non-specific interaction on aptamer-free MNP was minimized, whereas those of aptamer-immobilized MNP was enhanced. In this work, 2 important parameters in adsorption conditions were investigated; 1) The amounts of PQDEA@MNP used and 2) pH and types of buffer solutions.

Various weights of PQDEA@MNP were used to determine the amounts of the particles that can minimize BPA adsorption, indicating the minimized non-specific interaction. Increasing the weights of PQDEA@MNP seemed to enhance %BPA adsorbed. On the contrary, decreasing the weights of PQDEA@MNP from 1.00 mg to 0.10 mg tended to lower %BPA adsorbed (**Figure S4** in Supporting information). However, the use of PQDEA@MNP below 0.25 mg was troublesome in the separation step due to insufficient amounts of the particles in the magnetic separation process. Therefore, 0.25 mg of PQDEA@MNP was used in the later experiments.

The effect of pH and types of buffer solutions on BPA adsorption was then studied. Adsorption percentages of BPA on PQDEA@MNP were highly dependent on pH of buffer solutions because this can affect the surface charge of the particles, which essentially either improved or lessened their adsorption efficiency. Various pH (pH 7 - 10) and 2 types of buffer solutions (phosphate buffer and tris-HCl) with and without NaCl and tween-20 were used in the BPA adsorption experiments. It has been reported that the addition of sodium chloride and tween-20 was able to promote the selective adsorption of BPA on the solid support, so they were thus used in this work [48,49]. The results show that the adsorption of BPA on the particles in PBS buffer (pH 10) in the presence of NaCl and tween-20 seemed to favor the selective adsorption of BPA rather than the non-specific interaction, and this condition would be used in the later experiments (**Figure 6**). It was hypothesized that tween-20 might somewhat diminish the non-specific interaction between BPA and aptamer-free MNP, leading to the promotion of the selective adsorption of BPA with aptamer-immobilized MNP. Examples of the calculation of BPA adsorbed on the particles in different variations are shown in **Figures S5 - S7** in Supporting information.

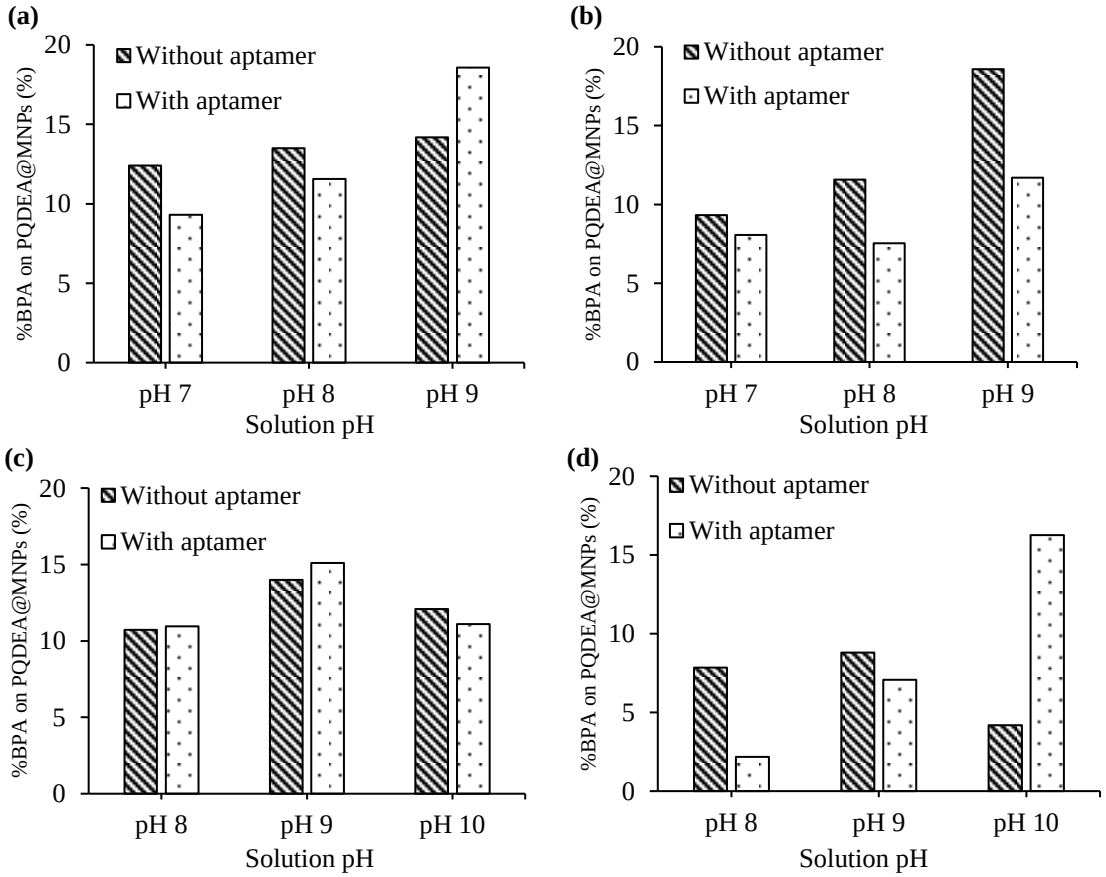

Figure 6 Adsorption percentages of BPA (0.25 ppm) on PQDEA@MNP (0.25 mg) in various pH in (a) tris-HCl buffer, (b) tris-HCl buffer with NaCl and tween-20, (c) PBS buffer and (d) PBS buffer with NaCl and tween-20. Noted that 150 mM NaCl and 0.1 %v/v tween-20 were used in these experiments.

Adsorption performance of aptamer-immobilized PQDEA@MNP

The CKSLENSYC peptide aptamer used in this work has been reported to specifically interact with BPA target [48,49]. To immobilize the aptamer on the particles, PQDEA@MNP and the aptamer were thoroughly mixed in deionized water to facilitate the ionic adsorption between the cationic polymer coated on the particle and the negative charge of the aptamer owing to the existence of the pendant carboxylate groups of glutamic acid (E) and cysteine (C) at 1 terminal of the aptamer. The chemical structure of BPA-specific peptide aptamer (CKSLENSYC) used in this work is shown in **Figure S8** in Supporting information. In addition, some other attractions between these 2 materials might exist, e.g. hydrogen bonding between unprotonated PDEAEMA units on MNP surface and the functional groups (-SH, NH_2, OH) presenting in the aptamer structure. Aptamer-immobilized PQDEA@MNP was then used for the adsorption experiments with BPA. **Figure S9** in Supporting information exhibits the linear relationship between the loaded concentration of BPA and the adsorbed BPA on the nano-adsorbents in the range of 0.04 - 0.20 ppm. Increasing the concentration of the loaded BPA led to the increase of those adsorbed on the particles. The adsorption percentages of BPA were in the range of 15 - 20 % of the loaded concentration. The narrow error bars with acceptable correlation coefficient (R^2 = 0.9927) signified the high reproducibility of the BPA adsorption efficiency of the nano-adsorbents. LOD of this study was 0.0145 ppm. The analytical performance of the particles was compared to those reported in previous works. It was apparent that the developed nano-adsorbents had comparable analytical performance to these reported works (**Table 1**).

Table 1 The comparison of the analytical performance of the particles from this work with those from other works.

Method	Analytical technique	Binding Unit	LOD	Reference
Label-free aptamer-functionalized MNP coated with cationic polymer	HPLC-FLD	Peptide aptamer	63.58 nM (0.0145 ppm)	This work
Aptamer-functionalized MNP	HPLC-DAD	DNA aptamer	4.38 and 8.76 nM[a] (1.0 and 2.0 ng/mL)	[43]
Label-free aptamer-functionalized molybdenum carbide nanotubes	Fluorescence	DNA aptamer	2 nM	[18]
β-cyclodextrin-functionalized ZnO QDs	Fluorescence	β-cyclodextrin	180 nM[a] (0.18 µM)	[54]
A nitrocellulose paper strip using molecularly imprinted nanoparticles	Fluorescence	Molecularly imprinted nanoparticles	192.299 nM[a] (43.9 µg/L)	[55]

Note: [a] the unit of LOD was converted from original papers to nM.

The selectivity towards BPA is an important parameter for aptamer-immobilized PQDEA@MNP. Many hypotheses have been proposed for the recognition of the aptamer towards the target, e.g. Van der Waals force, hydrogen bonding, electrostatic interaction, or stacking [47]. Therefore, to evaluate the selectivity to BPA of these particles, other compounds having similar molecular structure to BPA, including DHBP, BPS and BPAF, were used as interfering molecules. **Figure 7** shows the relative BPA signals of the dispersion when having only BPA in the solution (*A*) and those when mixing BPA with interfering compounds (*B*). The 1st bar exhibited the result of those when solely BPA used (without mixing with any interfering compounds), and the others were those when mixing BPA with the competitive compounds. The BPA signals in all cases were not significantly different, indicating that the presence of these BPA analogs did not disturb BPA adsorption on the particles. This result signified that these developed nano-adsorbents had high selectivity to BPA and good tolerance to interfering molecules. An example of the calculation of this result is shown in Supporting information.

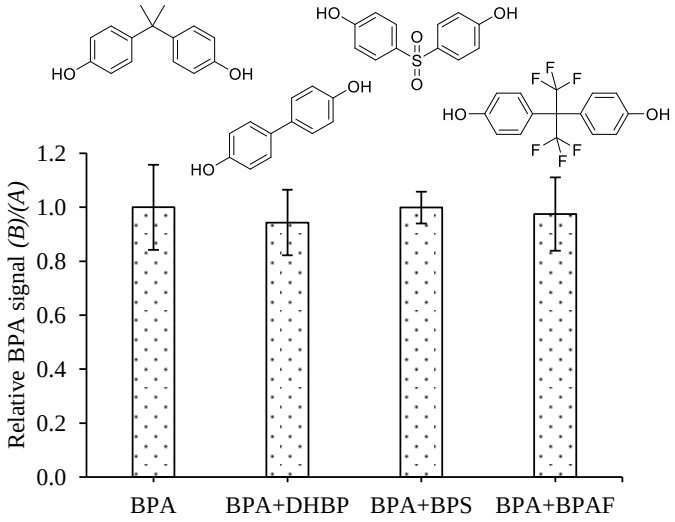

Figure 7 The effect of interfering molecules on BPA adsorption efficiency, where (*A*) is the BPA signals of the dispersion when having only BPA in the solution and (*B*) is those when mixing BPA with interfering compounds.

Conclusions

Magnetic nano-adsorbents coated with quaternized PDEAEMA and immobilized with BPA-specific peptide aptamer (CKSLENSYC) were developed. The particles were stable and well dispersible in water due to the polymer coating and showed high selectivity in adsorption with BPA due to the presence of the aptamer. The formation of MNP nanoclusters (30 - 60 nm in diameter) facilitated the magnetic separation process. Interestingly, these aptamer-immobilized particles retained their good BPA adsorption efficiency even when other compounds having similar chemical structures were present, indicating their good tolerance towards interfering molecules. This simple analysis with the use of the nano-adsorbents and no complicated molecular labelling step seems to be a promising approach for BPA analysis and might be applied for the analysis of other substances of interest.

Acknowledgements

This research was financially supported from National Research Council of Thailand (NRCT) (R2565B067). Jakkrit Tummachote especially thanks the Science Achievement Scholarship of Thailand (SAST) for the scholarship.

References

[1] J Muncke. Tackling the toxics in plastics packaging. *PloS Biol.* 2021; **19**, e3000961.
[2] MAB Siddique, SM Harrison, FJ Monahan, E Cummins and NP Brunton. Bisphenol A and metabolites in meat and meat products: Occurrence, toxicity, and recent development in analytical methods. *Foods* 2021; **10**, 714.
[3] L Chen, GR Shi, DD Huang, Y Li, CC Ma, M Shi, BX Su and GJ Shi. Male sexual dysfunction: A review of literature on its pathological mechanisms, potential risk factors, and herbal drug intervention. *Biomed. Pharmacother.* 2019; **112**, 108585.
[4] R Moreno-Gómez-Toledano. Relationship between emergent BPA-substitutes and renal and cardiovascular diseases in adult population. *Environ. Pollut.* 2022; **313**, 120106.
[5] JH Jun, JE Oh, JK Shim, YL Kwak and JS Cho. Effects of bisphenol A on the proliferation, migration, and tumor growth of colon cancer cells: *In vitro* and *in vivo* evaluation with mechanistic insights related to ERK and 5-HT3. *Food Chem. Toxicol.* 2021; **158**, 112662.
[6] MD Shelby. *NTP-CERHR monograph on the potential human reproductive and developmental effects of bisphenol A*. National Toxicology Program-Center of the Evaluation of Risks to Human Reproductions Monograph. 2008, p. 1-64.
[7] CA Richter, LS Birnbaum, F Farabollini, RR Newbold, BS Rubin, CE Talsness, JG Vandenbergh, DR Walser-Kuntz and FSV Saal. *In vivo* effects of bisphenol A in laboratory rodent studies. *Reprod. Toxicol.* 2007; **24**, 199-224.
[8] ZN Shehab, NR Jamil and AZ Aris. Modelling the fate and transport of colloidal particles in association with BPA in river water. *J. Environ. Manag.* 2020; **274**, 111141.
[9] PA Hunt, C Lawson, M Gieske, B Murdoch, H Smith, A Marre, T Hassold and CA VandeVoort. Bisphenol A alters early oogenesis and follicle formation in the fetal ovary of the rhesus monkey. *Proc. Natl. Acad. Sci. USA* 2012; **109**, 17525-30.
[10] FF Zafar, B Barati, H Rasoulzadeh, A Sheikhmohammadi, S Wang and H Chen. Adsorption kinetics analysis and optimization of Bisphenol A onto magnetic activated carbon with shrimp shell based precursor. *Biomass Bioenerg.* 2022; **166**, 106604.
[11] Y Zhang, ZL Yuan, XY Deng, HD Wei, WL Wang, Z Xu, Y Feng and X Shi. Metal-organic framework mixed-matrix membrane-based extraction combined HPLC for determination of bisphenol A in milk and milk packaging. *Food Chem.* 2022; **386**, 132753.
[12] FA Jahromi, F Moore, B Keshavarzi, SL Mohebbi-Nozar, Z Mohammadi, A Sorooshian and S Abbasi. Bisphenol A (BPA) and polycyclic aromatic hydrocarbons (PAHs) in the surface sediment and bivalves from Hormozgan Province coastline in the Northern Persian Gulf: A focus on source apportionment. *Mar. Pollut. Bull.* 2020; **152**, 110941.
[13] S Li, S Feng, AV Schepdael and X Wang. Hollow fiber membrane-protected amino/hydroxyl bifunctional microporous organic network fiber for solid-phase microextraction of bisphenols A, F, S, and triclosan in breast milk and infant formula. *Food Chem.* 2022; **390**, 133217.
[14] SC Cunha, T Inácio, M Almada, R Ferreira and JO Fernandes. Gas chromatography-mass spectrometry analysis of nine bisphenols in canned meat products and human risk estimation. *Food Res. Int.* 2020; **135**, 109293.

[15] Y Lei, Y Zhang, B Wang, Z Zhang, L Yuan and J Li. A lab-on-injector device with Au nanodots confined in carbon nanofibers for in situ electrochemical BPA sensing in beverages. *Food Control* 2022; **134**, 108747.

[16] Y Wang, Y Liang, S Zhang, T Wang, X Zhuang, C Tian, F Luan, SQ Ni and X Fu. Enhanced electrochemical sensor based on gold nanoparticles and MoS2 nanoflowers decorated ionic liquid-functionalized graphene for sensitive detection of bisphenol A in environmental water. *Microchem. J.* 2021; **161**, 105769.

[17] M Annalakshmi, TST Balamurugan, S Kumaravel, SM Chen and JL He. Facile hydrothermal synthesis of manganese sulfide nanoelectrocatalyst for high sensitive detection of bisphenol A in food and eco-samples. *Food Chem.* 2022; **393**, 133316.

[18] MQ He, K Wang, J Wang, YL Yu and RH He. A sensitive aptasensor based on molybdenum carbide nanotubes and label-free aptamer for detection of bisphenol A. *Anal. Bioanal. Chem.* 2017; **409**, 1797-803.

[19] LY Hu, CG Niu, Xy Wang, DW Huang, L Zhang and GM Zeng. Magnetic separate "turn-on" fluorescent biosensor for Bisphenol A based on magnetic oxidation graphene. *Talanta* 2017; **168**, 196-202.

[20] U Mahanitipong and M Rutnakornpituk. Palladium-immobilized polymer-coated magnetic nanocomposites as reusable catalysts for the reduction of 4-nitrophenol. *Polym. Int.* 2022; **71**, 1119-26.

[21] N Deepuppha, A Thongsaw, B Rutnakornpituk, WC Chaiyasith and M Rutnakornpituk. Alginate-based magnetic nanosorbent immobilized with aptamer for selective and high adsorption of Hg^{2+} in water samples. *Environ. Sci. Pollut. Res. Int.* 2020; **27**, 12030-8.

[22] M Hassanzadeh and M Ghaemy. Preparation of bio-based keratin-derived magnetic molecularly imprinted polymer nanoparticles for the facile and selective separation of bisphenol A from water. *J. Sep. Sci.* 2018; **41**, 2296-304.

[23] R Sahraei, K Hemmati and M Ghaemy. Adsorptive removal of toxic metals and cationic dyes by magnetic adsorbent based on functionalized graphene oxide from water. *RSC Adv.* 2016; **6**, 72487-99.

[24] N Deepuppha, S Khadsai, B Rutnakornpituk, U Wichai and M Rutnakornpituk. Multiresponsive poly (n-acryloyl glycine)-based nanocomposite and its drug release characteristics. *J. Nanomater.* 2019; **2019**, 8252036.

[25] K Hemmati, R Alizadeh and M Ghaemy. Synthesis and characterization of controlled drug release carriers based on functionalized amphiphilic block copolymers and super-paramagnetic iron oxide nanoparticles. *Polym. Adv. Technol.* 2016; **27**, 504-14.

[26] K Hemmati, A Masoumi and M Ghaemy. Tragacanth gum-based nanogel as a superparamagnetic molecularly imprinted polymer for quercetin recognition and controlled release. *Carbohydr. Polym.* 2016; **136**, 630-40.

[27] K Hemmati, R Sahraei and M Ghaemy. Synthesis and characterization of a novel magnetic molecularly imprinted polymer with incorporated graphene oxide for drug delivery. *Polymer* 2016; **101**, 257-68.

[28] PV Ostroverkhov, AS Semkina, VA Naumenko, EA Plotnikova, PA Melnikov, TO Abakumova, RI Yakubovskaya, AF Mironov, SS Vodopyanov, AM Abakumov, AG Majouga, MA Gin, VP Chekhonin and MA Abakumov. Synthesis and characterization of bacteriochlorin loaded magnetic nanoparticles (MNP) for personalized MRI guided photosensitizers delivery to tumor. *J. Colloid Interface Sci.* 2019; **537**, 132-41.

[29] EB Aydın, M Aydın and MK Sezgintürk. Determination of calreticulin using Fe_3O_4@ AuNPs core-shell functionalized with $PT(COOH)_2$ polymer modified electrode: A new platform for the impedimetric biosensing of cancer biomarkers. *Sens. Actuators B: Chem.* 2022; **367**, 132099.

[30] S Khadsai, N Seeja, N Deepuppha, M Rutnakornpituk, T Vilaivan, M Nakkuntod and B Rutnakornpituk. Poly(acrylic acid)-grafted magnetite nanoparticle conjugated with pyrrolidinyl peptide nucleic acid for specific adsorption with real DNA. *Colloids Surf. B Biointerfaces* 2018; **165**, 243-51.

[31] R Sahraei, T Shahalizade, M Ghaemy and H Mahdavi. Fabrication of cellulose acetate/Fe_3O_4@ GO-APTS-poly(AMPS-co-MA) mixed matrix membrane and its evaluation on anionic dyes removal. *Cellulose* 2018; **25**, 3519-32.

[32] R Sahraei, ZS Pour and M Ghaemy. Novel magnetic bio-sorbent hydrogel beads based on modified gum tragacanth/graphene oxide: Removal of heavy metals and dyes from water. *J. Clean. Prod.* 2017; **142**, 2973-84.

[33] S Meerod, N Deepuppha, B Rutnakornpituk and M Rutnakornpituk. Reusable magnetic nanocluster coated with poly(acrylic acid) and its adsorption with an antibody and an antigen. *J. Appl. Polym. Sci.* 2018; **135**, 46160.
[34] S Paenkaew, T Kajornprai and M Rutnakornpituk. Water dispersible magnetite nanocluster coated with thermo-responsive thiolactone-containing copolymer. *Polym. Adv. Technol.* 2020; **31**, 1349-55.
[35] T Theppaleak, G Tumcharern, U Wichai and M Rutnakornpituk. Synthesis of water dispersible magnetite nanoparticles in the presence of hydrophilic polymers. *Polym. Bull.* 2009; **63**, 79-90.
[36] P Theamdee, R Traiphol, B Rutnakornpituk, U Wichai and M Rutnakornpituk. Surface modification of magnetite nanoparticle with azobenzene-containing water dispersible polymer. *J. Nanopart. Res.* 2011; **13**, 4463-77.
[37] B Rutnakornpituk, U Wichai, T Vilaivan and M Rutnakornpituk. Surface-initiated atom transfer radical polymerization of poly (4-vinylpyridine) from magnetite nanoparticle. *J. Nanopart. Res.* 2011; **13**, 6847-57.
[38] J Tummachote, M Rutnakornpituk, D Channei, F Kielar and B Rutnalornpituk. Amino-containing polymer-coated magnetite nanoparticles as nano-adsorbents for bisphenol A: Synthesis, kinetic and thermodynamic study. *J. Met. Mater. Miner.* 2022; **32**, 11-23.
[39] N Deepuppha, A Kadnaim, B Rutnakornpituk and M Rutnakornpitak. Poly(ester urethane)-crosslinked carboxymethylchitosan as a highly water swollen hydrogel. *J. Met. Mater. Miner.* 2020; **30**, 48-56.
[40] M Hassanzadeh and M Ghaemy. An effective approach for the laboratory measurement and detection of creatinine by magnetic molecularly imprinted polymer nanoparticles. *New J. Chem.* 2017; **41**, 2277-86.
[41] S Khadsai, N Seeja, M Rutnakornpituk, T Vilaivan, M Nakkuntod, W Suwankitti, F Kielar and B Rutnakornpituk. Selective enrichment of zein gene of maize from cereal products using magnetic support having pyrrolidinyl peptide nucleic acid probe. *Food Chem.* 2021; **338**, 127812.
[42] W Inthanusorn, M Rutnakornpituk and B Rutnakornpituk. Reusable poly(2-acrylamido-2-methylpropanesulfonic acid)-grafted magnetic nanoparticles as anionic nano-adsorbents for antibody and antigen. *Int. J. Polym. Mater. Polym. Biomater.* 2022. DOI: 10.1080/00914037.2022.2042288.
[43] Y Su, C Shao, X Huang, J Qi, R Ge, H Guan and Z Lin. Extraction and detection of bisphenol A in human serum and urine by aptamer-functionalized magnetic nanoparticles. *Anal. Bioanal. Chem.* 2018; **410**, 1885-91.
[44] T Theppaleak, M Rutnakornpituk, U Wichai, T Vilaivan and B Rutnakornpituk. Anion-exchanged nanosolid support of magnetic nanoparticle in combination with PNA probes for DNA sequence analysis. *J. Nanopart. Res.* 2013; **15**, 2106.
[45] S Ye, R Ye, Y Shi, B Qiu, L Guo, D Huang, Z Lin and G Chen. Highly sensitive aptamer based on electrochemiluminescence biosensor for label-free detection of bisphenol A. *Anal. Bioanal. Chem.* 2017; **409**, 7145-51.
[46] ZS Beiranvand, AR Abbasi, S Dehdashtian, Z Karimi and A Azadbakht. Aptamer-based electrochemical biosensor by using Au-Pt nanoparticles, carbon nanotubes and acriflavine platform. *Anal. Biochem.* 2017; **518**, 35-45.
[47] S Beiranvand and A Azadbakht. Electrochemical switching with a DNA aptamer-based electrochemical sensor. *Mater. Sci. Eng. C* 2017; **76**, 925-33.
[48] IK Yoo and WS Choe. Screening of peptide sequences with affinity to bisphenol A by biopanning. *Korean J. Microbiol.* 2013; **49**, 211-4.
[49] J Yang, SE Kim, M Cho, IK Yoo, WS Choe and Y Lee. Highly sensitive and selective determination of bisphenol-A using peptide-modified gold electrode. *Biosens. Bioelectron.* 2014; **61**, 38-44.
[50] SH Sadr, S Davaran, E Alizadeh, R Salehi and A Ramazani. PLA-based magnetic nanoparticles armed with thermo/pH responsive polymers for combination cancer chemotherapy. *J. Drug Deliv. Sci. Technol.* 2018; **45**, 240-54.
[51] VH Nguyen, Y Haldorai, QL Pham and JJ Shim. Supercritical fluid mediated synthesis of poly(2-hydroxyethyl methacrylate)/Fe_3O_4 hybrid nanocomposite. *Mater. Sci. Eng.: B* 2011; **176**, 773-8.
[52] J Moon, S Oh, T Kang, S Hong and J Yi. Investigation of adsorption behavior of bisphenol A on well fabricated organic surfaces using surface plasmon resonance spectroscopy. *J. Nanosci. Nanotechnol.* 2006; **6**, 3543-6.
[53] H Du, S Shi, W Liu, G Che and M Piao. Hydrophobic-force-driven adsorption of bisphenol A from aqueous solution by polyethylene glycol diacrylate hydrogel microsphere. *Environ. Sci. Pollut. Res. Int.* 2019; **26**, 22362-71.

[54] VV Kadam, RM Balakrishnan and JP Ettiyappan. Fluorometric detection of bisphenol A using β-cyclodextrin-functionalized ZnO QDs. *Environ. Sci. Pollut. Res.* 2021; **28**, 11882-92.
[55] R Üzek, E Sari, S Şenel, A Denizli and A Merkoçi. A nitrocellulose paper strip for fluorometric determination of bisphenol A using molecularly imprinted nanoparticles. *Microchim. Acta* 2019; **186**, 218.

Appendix

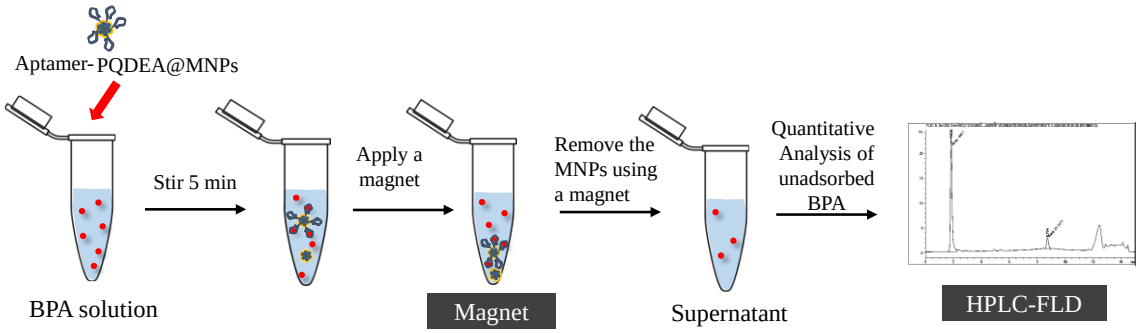

Figure S1 BPA adsorption experiments using aptamer-immobilized PQDEA@MNP and the determination of the adsorbed BPA on the particle *via* HPLC-FLD.

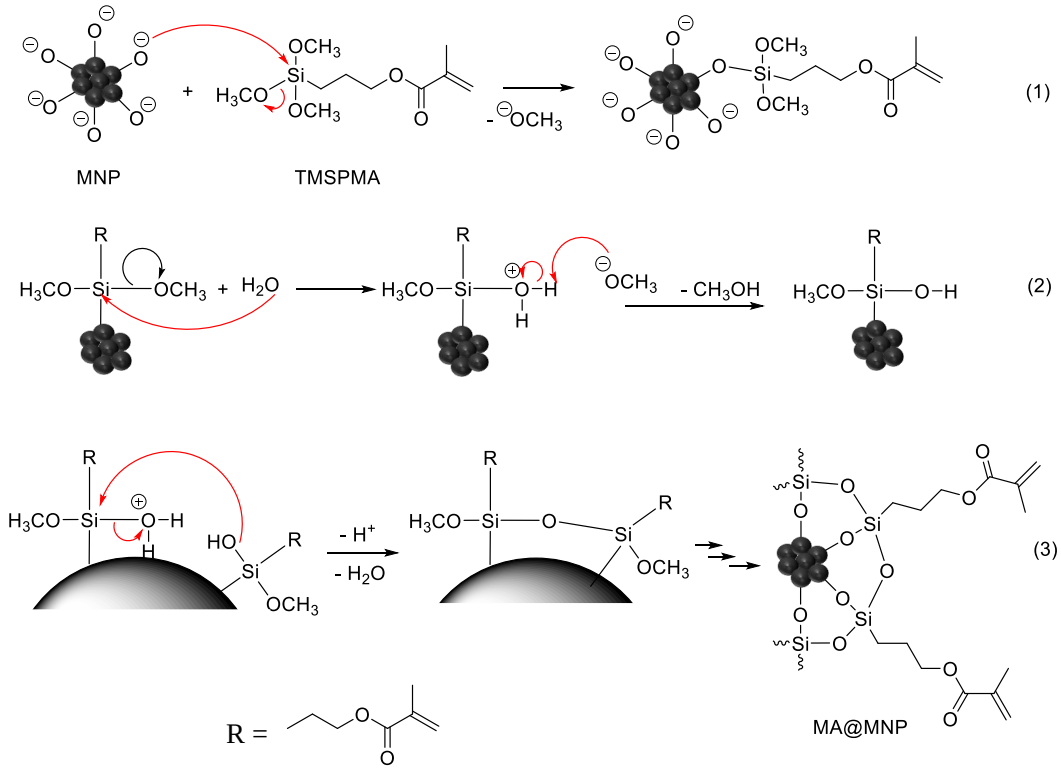

Figure S2 The proposed mechanism of the silica layer formation on MNP surface 1) the reaction between Fe-O^- and TMSPMA, 2) the reaction of TMSPMA-immobilized MNP with water to form silanol, 3) the reaction between two neighboring silanols to form silica layer on MNP surface.

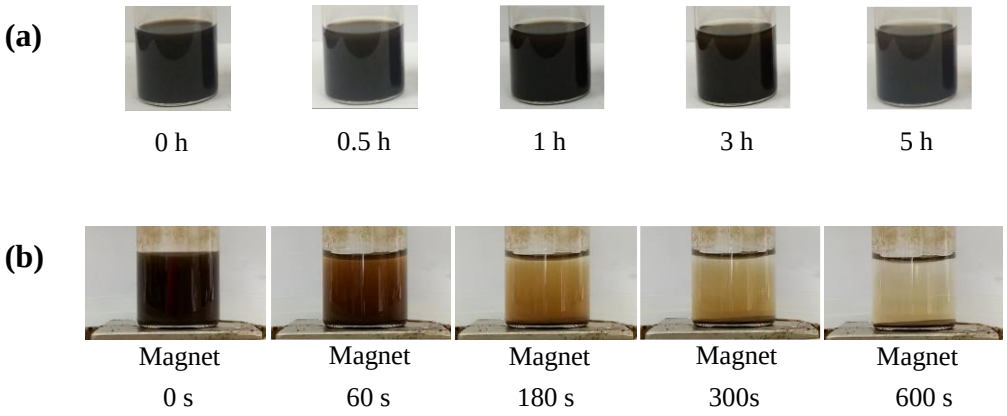

Figure S3 (a) The stability in water and (b) magnetic separation ability of PQDEA@MNP.

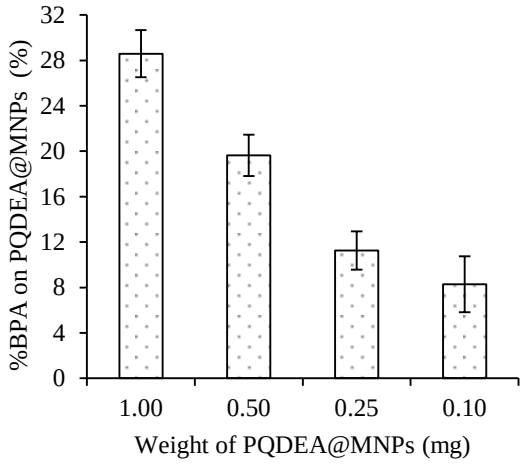

Figure S4 Adsorption percentages of BPA using various weights of PQDEA@MNP. Noted that 1.0 ppm of BPA in PBS buffer with NaCl and tween-20 was used in all these experiments.

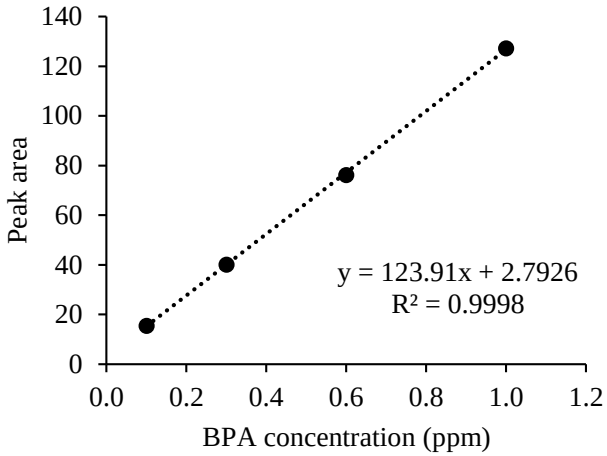

Figure S5 The standard curve of BPA for this study.

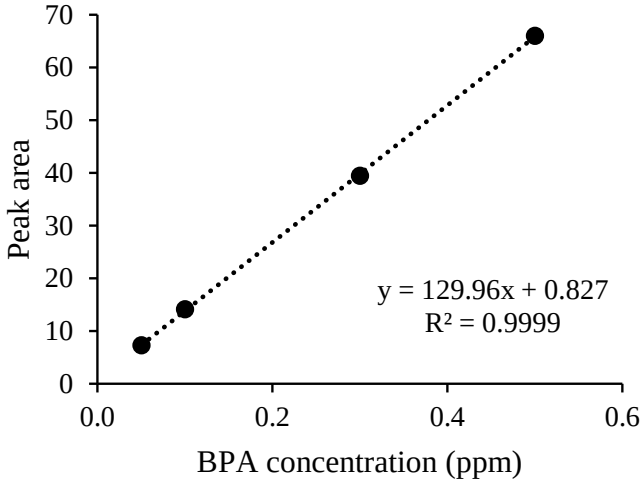

Figure S6 The standard curve of BPA for this study.

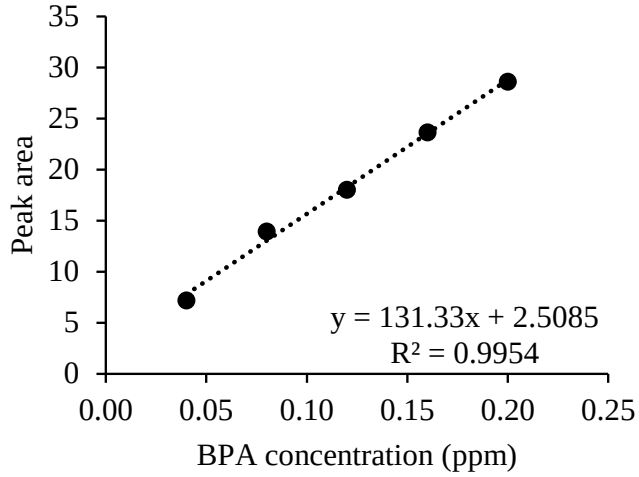

Figure S7 The standard curve of BPA for this study.

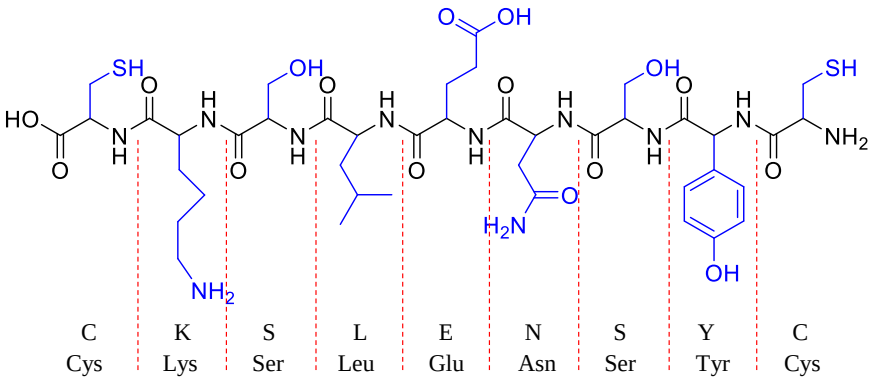

E – Glutamic acid

C – Cysteine

K – Lysine

S – Serine

L – Leucine

N – Asparagine

Y – Tyrosine

Figure S8 The chemical structure of BPA-specific peptide aptamer (CKSLENSYC) used in this work.

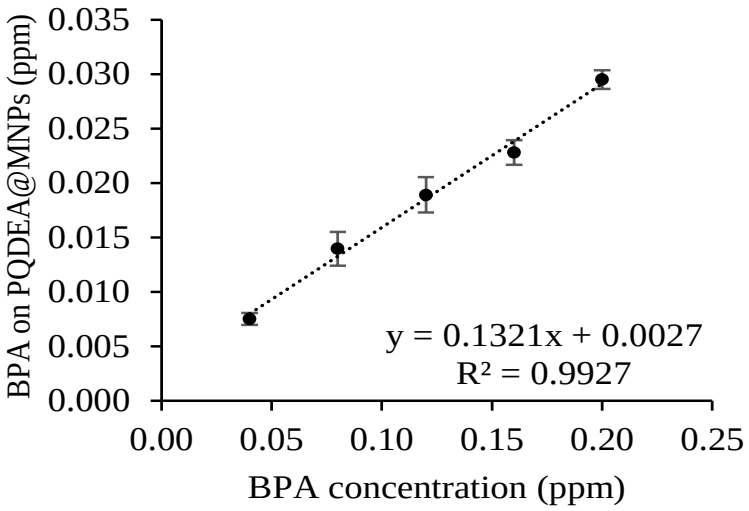

Figure S9 The plot showing the linear relationship between BPA adsorbed on aptamer-immobilized PQDEA@MNP (0.25 mg) and the loaded concentration of BPA in the 0.04-0.20 ppm range. The experiments were performed in PBS buffer (pH 10) with 150 mM NaCl and 0.1%v/v tween-20.